FOCUS HISTORY OF THE HUBBLE SPACE TELESCOPE - LAUNCH TO MAY 1993 [1]

H. Hasan

Space Telescope Science Institute, 3700 San Martin Dr., Baltimore, MD 21218
Electronic mail: hasan@stsci.edu

C. J. Burrows

Space Telescope Science Institute and European Space Agency
Electronic mail: burrows@stsci.edu

D. J. Schroeder

Beloit College, Department of Physics, Beloit, WI 53511
Electronic mail: schroeder@beloit.edu

[1]Based on observations with the NASA/ESA *Hubble Space Telescope*, obtained at the Space Telescope Science Institute, which is operated by the Association of Universities for Research in Astronomy, Inc., under NASA Contract No. NAS5-26555.

ABSTRACT

Since the launch of the Hubble Space Telescope (HST) the secondary mirror of the telescope has been moved several times in order to collimate the telescope and also to define a position of best focus. In addition to these moves the focus position changes over time because of water desorption by the graphite epoxy in the metering truss. We report here the focus history of the telescope based on a knowledge of the mirror moves made and an analysis of desorption monitoring data obtained by the Faint Object Camera (FOC) in the F/96 mode and of the routine calibration data obtained by the Wide Field and Planetary Cameras. Focus values were extracted using two different methods. In the first method the distance between the center of the Point Spread Function (PSF) and the shadows of the pads supporting the HST primary mirror are related to the focus error. In the second method an analytical formula for the PSF with variable aberration coefficients is fitted to the data. Focus positions derived from the two methods show good agreement.

The data show that a desorption of about 83 microns has taken place since Aug. 16, 1990. The desorption has clearly not levelled off as expected from the trend of the earlier data. Long term variations of the secondary mirror position of $\sim 3 - 15$ microns from the "best" focus position have been observed. Variations of the order of $2 - 5$ microns over an orbital period have also been noted. Focus changes resulting from secondary mirror movements greater than ~ 5 microns changes the point spread function significantly and makes deconvolution and quantitative measurements difficult.

1. INTRODUCTION

The Optical Telescope Assembly (OTA) in the Hubble Space Telescope (HST) consists of a 2.4 m aperture $F/24$ Ritchey-Chrètien telescope. It is now well established that the telescope suffers from spherical aberration and that no choice of focal plane yields the diffraction limited images that the telescope was designed to produce. Since the spherical aberration in the HST primary mirror causes different parts of the beam to converge at different points, there is no well defined focal point. Nevertheless, criteria can be set up to determine a "best" focus position for the telescope. Maintenance of the focus of the telescope is important for the present state of HST, since departures of more than ~ 5 microns (corresponding to ($\sim 1/20$ th wave of focus error at 6328 Å) change the point spread function (PSF) significantly and make deconvolution and quantitative measurements difficult.

In April, 1991 a panel of optics experts (Optical Alignment Panel) was set up by the Project and was assigned the task of identifying a suitable focus position for the telescope. The definition of "best" or "optimal" focus initially adopted was that position of the OTA secondary mirror that gives the maximum encircled energy in a 0.1 arcsec radius of a stellar image in the Faint Object Camera (FOC) (at the internal FOC focus position at launch) at 4860 Å(Schroeder, 1991). From simulations, this secondary mirror position corresponds to a shift in the focal plane from paraxial focus of 12.2 mm (paraxial focus is nominally at 1500.128 mm from the OTA primary mirror). This position is a compromise for the cameras (Wide Fieldand Planetary Camera (WFPC) and FOC) and the spectrographs (Faint Object Spectrograph and Goddard High Resolution Spectrograph), for which we know from simu-

lations that the throughput in the small apertures is greater for positions of the secondary mirror closer to the primary mirror than the "best focus" position.

In order to establish the best focus and to put the mirror at this position, on October 18, 1991 a series of FOC F/96 images were taken at various positions of the secondary mirror ("focus sweep"). The OTA secondary mirror position as determined by these data was about 5 microns too close to the primary mirror (Jedrzejewski 1991). As this position is very close to the nominal best focus and considerable calibration data had already been obtained at this focus setting, it was subsequently decided to maintain the OTA focus at this position. In order to avoid frequent moves of the secondary mirror, our present aim is to maintain the telescope focus to within 0.55 mm of this position or equivalently a motion of 5 microns of the secondary mirror. In the past this goal has not been achieved. However, we are able to reconstruct the average focus history to the desired accuracy *post facto*. The relationship between a move $\Delta(PF)$ of the focal plane to the corresponding move $\Delta(SM)$ of the secondary mirror, in the same coordinate system, is computed from the standard relation for a Cassegrain system (Schroeder, 1987):

$$\Delta(PF) = m^2\Delta(SM) = -109\Delta(SM) \tag{1}$$

where $m = F/F_1 = 24./2.3 = 10.435$ is the magnification of the secondary mirror. Here F and F_1 ar the $F - numbers$ of the OTA and the primary mirror respectively.

The focus position changes over time because of water desorption of the graphite epoxy in the metering truss that causes the secondary mirror to move. In addition, a $2 - 5$ micron

movement of the secondary over short periods of time has been observed in both FOC and WFPC images. The cause for this change, commonly referred to as OTA "breathing," is not understood. One case of "heavy breathing" in which a secondary mirror movement of $\sim$ 10 microns between a WF and a PC exposure taken $\sim$ 2.5 hrs. apart has also been detected.

An Observatory Level Test (OLT) to monitor desorption was devised during the Science Verification (SV) phase of HST and has been periodically executed since then (the interval between tests at present is 12 weeks). Analysis of these data through January 1993 showed that the OTA had desorbed a total of about 83 microns, but at a decreasing rate, since August 16, 1990. A best fit curve through the data indicates that the OTA will shrink another $\sim$ 8 microns by August 1993. The secondary is moved back to a position within 5 microns of the October 18, 1991 focus position to correct for the desorption. In order to minimize the secondary mirror moves, the plan is to apply an overcorrection so that further desorption will cause the mirror to move towards the desired focus position. The last mirror move to correct for desorption was made on November 25, 1992. If the desorption continues along the present trending curve another move will not be required till August, 1993.

Here we report the results of the FOC F/96 desorption test as well as results of monthly focus measurements on WF and PC images taken from the stellar monitoring program. Although the WF and PC data are of a poorer quality than the FOC data, both because the signal to noise is lower and because these images are undersampled, they have been analysed to provide trending information since September 1991.

The history of OTA secondary mirror actuator movements is available on the Space Telescope Electronic Information System (STEIS) in the directory software/tim. A table of

the major mirror moves affecting scientific observations is given in section 2.

2. MIRROR MOVE HISTORY

There have been a total of 215 mirror adjustments since launch, mainly for engineering purposes. The 13 moves affecting scientific observations are listed in Table 1. The last six columns of the table give the secondary mirror position relative to the launch position, in physical units (microns of translation and arcseconds of tilt). The OTA coordinate system (V1, V3, V2) is used here. The V1 axis is along the HST optical axis, and together with the (V2, V3) axes forms a right handed system with the focal plane lying in the (V2, V3) plane. Translations (DX, DY, DZ) are along the (V1, V3, V2) axes, respectively, while the tilts (TX, TY, TZ) are about (-V1,+ V2, -V3) respectively. The effect of desorption, which is estimated from the results of the focus test, is not included in Table 1. The telescope has been routinely maintained at the same collimation (secondary mirror tilt and decenter) since day 351 in 1990, with only focus variations ever since. This collimation setting was first used on day 323 in 1990 and is, therefore, generally known as the "day 323" position. The only exceptions are the period between days 81 and 96 in 1991 and periods in which alignment testing was being done and no science data was taken. After each collimation excursion, the secondary mirror was repositioned to high accuracy at the "day 323" position. The "day 323" position is known to have some misalignment associated with it corresponding to about 1/15 th waves of coma at 6328 Å. This coma will be removed with a secondary mirror move after the servicing mission scheduled for December 1993.

3. METHOD OF ANALYSIS

Initially, two methods were used to measure the focus position of the OTA—the "pad method" developed by Schroeder (1991) and "phase retrieval." Both methods showed good agreement and are outlined below, though the pad method is used for routine analysis because of its simplicity.

3.1. Pad Method

The "pad method" is based on the observation that the diffraction shadows of the three pads supporting the OTA primary mirror (PM) (Figure 1) are clearly seen in any well-exposed stellar image. These pad images, seen as "bright spots," are the so-called Arago or Poisson spot seen behind any circular obstacle. The method consists simply of displaying the image, measuring the distance r from the center of each spot to the image peak, and using the average $< r >$ to find the distance $\Delta(PF)$ from paraxial focus to the focal surface of the OTA. The spot centers are measured in detector coordinates and then converted to OTA distances using the known scale factor for the camera.

The distance between the pad images varies with focus, as shown schematically in Figure 2. The relation between $< r >$ and $\Delta(PF)$ or, the corresponding shift $\Delta(SM)$ of the secondary mirror (SM) from its nominal position, is most easily derived by ray-tracing. Other optical changes such as those in the radius of curvature of the primary mirror can lead to focus changes. There is no practical way to distinguish the cause of focus shift. In this approach we take the as-built OTA and trace rays from the centers of the pads on the PM to the image surface for several SM positions. The traces are done for a star on the OTA

axis, hence only spherical aberration (SA) and defocus determine $< r >$. Our assumption is that each pad spot in an image is centered on the geometric ray through the corresponding pad center.

The average position of rays traced through the pad is displaced by 2.8 microns from the ray at the pad center, which corresponds to only 1.4 microns of OTA secondary mirror motion. The as-built parameters of the OTA are as follows: PM: radius of curvature= 11041.7 mm, conic constant $K = -1.0139$, distance to SM = 4906.889 mm; SM: radius of curvature = 1358.065 mm, conic constant $K = -1.496$, distance from PM vertex to focal surface = 1500.128 mm. The PM-SM separation above corresponds to $\Delta(PF) = \Delta(SM) = 0$. Taking the coordinates of the pad centers from Figure 1, we get the results in the Table 2.

The positive displacements $\Delta(SM)$ in this table are away from the PM. Positive $\Delta(SM)$ decreases the PM to paraxial focus distance. On the OTA instrumental aperture plane, which is fixed relative to the primary mirror, positive $\Delta(SM)$, therefore, corresponds to an image closer to marginal focus.

Using the data in the two left columns in Table 2, we get the following relation between $< r >$ and $\Delta(SM)$.

$$< r > (microns) = 596.5 - 1.998\Delta(SM)(microns) \qquad (2)$$

A conversion from $< r >$ in microns to $< r >$ in pixels can be made by using the camera scale projected on the $F/24$ focal plane as follows. From the OTA scale of 3.581 milliarcsec/micron and the FOC F/96 scale of 24.4 milliarcsec/pixel, we get a

conversion factor of 6.812 micron/FOC pixel at the $F/24$ OTA focus. (N.B. The geometric correction algorithm applied by the pipeline when processing early FOC F/96 data gave a scale of 24.4 milliarcsec/pixel rather than 22 milliarcsec/pixel. We continue to process our data in the same way in order to maintain consistency between measurements.) When this conversion factor is applied to Equation (2) we get

$$< r > (pixels) = 87.57 - 0.2933\Delta(SM)(microns) \quad (3)$$

The corresponding conversion factors for PC and WFC are based on scales of 43 and 100 milliarcsec/pixel and give the equations, respectively:

$$< r > (pixels) = 49.7 - 0.1665\Delta(SM)(microns) \quad (4)$$

$$< r > (pixels) = 21.4 - 0.0716\Delta(SM)(microns) \quad (5)$$

The results in Table 2 can also be derived by another approach. The transverse spherical aberration (TSA) is computed as product of the OTA focal length and the change in slope of the nominal optical path difference (OPD) between an aberrated ray and the chief ray (the ray that goes through the optical center of the system). The difference between TSA and pad radius $< r >$ is then related to $\Delta(SM)$ by simple geometric means (Burrows et al., 1991). Ray tracing is preferred, however, for two reasons. First, the SA of the as-built OTA depends on the PM–SM separation; over the range of SM displacement in the table there is a change of about one percent in third-order SA. Second, the as-built OTA has a residual

fifth-order SA not present in the OTA as designed. These two factors are automatically accounted for when rays are traced, but must be explicitly included if the OPD approach is used, although ray trace shows them to be small. A comparison of results obtained using Equation 3 and the corresponding equation using the OPD approach are shown on columns 2 and 3 of Table 3.

3.2. Phase Retrieval Method

In this method a theoretical model of the PSF is fitted to the data. The theoretical model and fitting procedure are described below.

3.2.1. Theoretical PSF Model

The optical path difference between a particular ray and the chief ray (the ray that goes through the optical center of the system) may be expressed in terms of polynomials. An appropriate set of polynomials used for this purpose was developed, for a circular aperture with a centered circular obscuration, by Zernike (1934), since each term of the polynomial represents a particular optical distortion (Seidel aberration) of the system. The expansion coefficients give the "strength" of the aberration. Thus, for an unaberrated beam all the coefficients will be zero. The OPD or wavefront error, $F(r,\theta)$, at any point (r,θ) may be expanded in terms of Zernike polynomials, $Z_i(r,\theta)$ as (Born and Wolf, 1965):

$$F(r,\theta) = \sum_{i=1}^{N_{max}} a_i Z_i(r,\theta) \tag{6}$$

From Fourier optics, spread of light at the image is determined both by the wavefront

error and the geometry of the beam in the exit pupil. The **amplitude spread function** (ASF), which quantifies this light distribution mathematically, is the Fourier Transform of the **pupil function** $P(r,\theta)$, given by

$$P(r,\theta) = A(r)O(r,\theta+\omega)e^{ikF(r,\theta)}, \tag{7}$$

where λ is the wavelength of light, $k = 2\pi/\lambda$ is the wave number, and $O(r,\theta+\omega)$ takes into account the obscuration of the light beam. The angle, ω gives an overall rotation of the obscurations with respect to detector coordinates. For the OTA, in addition to the central obscuration, the beam has obscurations caused by the spider supports of the secondary mirror and the primary mirror pads (Figure 1).

The PSF is determined as the modulus squared of the ASF. Effects of low order aberrations caused by irregularities in the OTA primary mirror surface and HST jitter may be modelled by modifying $F(r,\theta)$ and the ASF respectively.

3.2.2. Fitting Procedure

We minimize a merit function which is the RMS difference between a simulated and observed PSF, using a non - linear fitting routine CURFIT (Bevington, 1969) by varying the coefficients for focus and spherical aberration. This method allows an independent estimate of spherical aberration and focus, unlike the pad method which gives focus for an assumed amount of spherical aberration.

The aberration coefficient Z_4 corresponds to a focus error which can be shown by geo-

metric arguments to correspond to a SM displacement, $\Delta(SM)$ by

$$\Delta(SM) = (Z_4^c - Z_4^p)(3.887 \times 8F^2)/110 \quad (8)$$

where $\Delta(SM)$ is expressed in microns as before, Z_4^c and Z_4^p are the focus error at the focus position being measured and paraxial focus respectively, $F = 24 \times 0.9984$ is the actual OTA image space focal ratio at paraxial focus. At paraxial focus the wavefront error is proportional to r^4. Thus Z_4^p may be easily computed by equating the r^2 term in the orthogonal expansion of spherical aberration to the r^2 term from the focus polynomial with coefficient Z_4. For the OTA we get $Z_4^p = -1.249$ microns.

3.3. Comparison of Pad Method and Phase Retrieval Method

A comparison of the values for $\Delta(SM)$ obtained by the pad method and the phase retrieval method for some representative FOC F/96 images are shown in Table 3. The first two lines of this table show the results for images, which were simulated for $\Delta(SM) = 105.9$ microns and $\Delta(SM) = 100.9$ microns respectively, while the last three lines give results for observed images. Columns 2 and 3 show the results obtained using the OPD method and Equation 3 respectively, of measurements of pad positions made by one of us (HH). Column 4 shows the same measurements made by another of us (DJS) and using Equation 3. Finally, column 5 shows the results of the phase retrieval method.

Both the pad method and the phase retrieval method give good agreement in measuring relative focus changes. The difference in the absolute value of $\Delta(SM)$ between the two methods is ~ 7 microns; the phase retrieval method gives a consistently smaller value. This

constant bias is due to the fact that the pad method relies on the judgement of the human eye to centroid the pad image. For this reason an inter-personal bias appears as is evident when comparing results measured by two different people (columns 3 and 4). The reproducibilities of $\Delta(SM)$ caused by variations in repeated measurements of the pad centers in a single FOC image is ± 3 microns. The phase retrieval method is generally more reliable and bias free. However, when the image has a great deal of jitter (as was the case in Image 3 of Table 3), the phase retrieval method does not converge to a very good value. A sanity check on either method is to blink successive images to estimate focus changes. To an experienced eye, gross errors become very apparent. For the phase retrieval method, blinking the data and fitted image also gives a good estimate of whether the method has converged well or not.

4. RESULTS

4.1. Analysis of FOC data

The FOC desorption monitoring test is four 15 min images of the spectrophotometric standard star, GRW+70d 5824 through the filter F486N using the FOC F/96. The four images are co-added to improve the signal to noise ratio. The data were analysed by the pad method and is plotted together with fits in Figure 3. Initial fits to the available data (till November 20, 1991) indicated that the OTA was desorbing according to the formula

$$d = 63.4 - 115.6e^{-t/185.5} \tag{9}$$

where d is the desorption in microns since August 16, 1990 and t is the number of days since April 24, 1990 (HST launch). Subsequent data did not follow this curve and another fit was done (data till May 19, 1992) leading to the formula

$$d = 81.7 - 110.0e^{-t/322.7} \tag{10}$$

The test done on October 6, 1992 indicated that this formula was still not good enough to predict the OTA desorption. The last fit gave the formula

$$d = 106.5 - 100.6e^{-t/716.7} - 131.5e^{-t/61.5} \tag{11}$$

Figure 3 shows a plot of the measurements and the best fit curves for data available till

November 20, 1991 (dashed curve), May 19, 1992 (dot-dashed curve) and October 6, 1992 (dotted curve). There is a large difference between the curves beyond November 20, 1991. The desorption has clearly not leveled off as suggested by the first fitted curve with the smallest time constant. Results of the latest desorption test on January 26, 1993 indicate that the desorption continues along the last fitted curve.

A mirror move of 14 microns to counter desorption was made on August 23, 1992. This move, which was based on a fit to the data available through May 19, 1992 (dot-dashed curve in Figure 3), fell $\sim$ 3 micron short of the October 18, 1991 position. Another move of 10 microns was made on November 25, 1992 to overcorrect the focus by $\sim$ 3 micron. Desorption will cause the focus to slowly drift to the October 18, 1991 postion without frequent mirror moves.

Figures 6 and 7 show the reference positions for October 18, 1991 as well as the moves made to counter desorption. Table 4 lists the dates of the desorption tests and results of the measurements.

4.2. Analysis of PC data

Data from the PC stellar monitoring proposals was analyzed for the period September 13, 1991 through March 23, 1993. In this test a standard star was exposed for 1.2 secs on chip PC6, using a series of filters. The images most suitable for focus analysis were the ones through the F439W filter because in this bandpass the pad images are clearest. It should be mentioned that these are not very well exposed images so the pad positions are not easy to measure. Because of this and of the undersampling of WFPC images the uncertainties

are larger than in the case of the FOC data. The images were displayed and the positions of the pads 2 and 3 measured. Pad 1 was not clearly visible in most images as it falls in the shadow of the OTA spider in PC6. The uncertainties in its measurements are expected to be larger than in the other two cases. Values of $\Delta(SM)$ were computed from equation (4) and are overplotted with the FOC data in Figure 4 after adjusting for an apparent focus difference of $\sim$ 8 microns between the FOC and PC. In each case, five measurements were made for each image from which 1σ values were computed and plotted as error bars. These data are also overplotted with the FOC data in Figure 6 together with the mirror moves made to counter desorption.

There is a great deal of scatter in the data but it does to follow the general trend of the FOC data.

4.3. Analysis of WF data

The WF data were taken from the same proposals as the PC data above and analysed as described in section 4.2. The exposures were 0.6 secs on chip W2. Only the positions of pads 2 and 3 were measured, since pad 1 was barely visible. The results are overplotted with the FOC data in Figures 5 and 7 with an arbitrary normalization. There is a global shift of $\sim$ 6 microns (or $\sim$ 1/20 th wave of focus error at 6328 Å) between the normalization of the WF and PC data. Similar offsets in focus between the WF and PC cameras in WFPC2 have been seen in global tests. The WF data also follow the general trend of the FOC and PC data.

5. OTA "BREATHING"

Each set of FOC data contains several exposures, and the focus measurements reported above were made on the sum of the exposures. However, within some sets show $2 - 5$ microns of focus variation which are not attributable to measurement errors. This short period variability is referred to as OTA "breathing". Such focus variations on an orbital time scale have also been seen in WF and PC data.

A test designed to measure focus changes on an orbital scale was executed on December 25, 1992. In this test, 34 images were taken in PC5 over 6 HST orbits with the target in the continuous viewing zone (CVZ). Results of the pad measurements on these images are plotted in Figure 9 and indicate ~ 3 microns focus changes (in terms of $\Delta(SM)$ movement) between most of the images with the largest departure being ~ 7 microns (blinking the images indicates that the largest error is ~ 5 microns). The breathing appears to be erratic and the cause is not yet known, though there is some indication that orbital variations of the focus may be thermally induced.

Over periods of months, the WFPC stellar monitoring data (Figures 4 and 5) show significant and larger departures from the best fit line as plotted in Figure 8. There is generally good correlation between the PC and WF residuals. (One anomalous case exists on Nov. 4, 1992 when a difference of ~ 10 microns was found between the PC and WF data.)

Departures from the best fit line plotted in Figure 8 show long term focus variations of $\sim 3 - 15$ microns. Since the WF and PC data are well correlated, and the amplitude is

larger than that associated with the orbital breathing, this large range of focus variations is probably caused by a focus offset (about which breathing may occur) which is dependent of the sun-earth-hst-target geometry.

The picture that emerges from these results is that there is a short term (over an orbital period) focus variation of $\sim 3-5$ microns (though occasionally a bigger effect has been seen), and a larger one of $\sim 3-15$ microns which may be pointing dependent. From simulations we know that "breathing" of $3-5$ microns would not significantly degrade the WFPC2 or COSTAR images and corresponds to at most 1/20 th RMS wavefront error at 6328 Å, and to a loss of central intensity of $\sim 5\%$ at 6328 Åand $\sim 30\%$ at 2000 Å. For the spectrographs, a 5 micron focus change does not affect the throughput for the large (1" $\times$ 1") aperture and causes $< 1\%$ change for the small (0.25" $\times$ 0.25") aperture. Focus variations greater than 5 microns would have a somewhat detrimental effect on scientific observations. However, since the larger variations may be related to HST pointing , and relatively uncommon, they are unlikely to have a serious impact on an individual scientific program. A better understanding of the effect must be achieved however, as it could be largely avoided by changing the HST scheduling after the refurbishment mission scheduled for December 1993.

6. CONCLUSION

Analysis of the desorption data from August 16, 1990 through January 26, 1993 shows that the OTA has desorbed ~ 83 microns according to the formula

$$d = 106.5 - 100.6e^{-t/716.7} - 131.5e^{-t/61.5} \tag{12}$$

where d is the desorption in microns since August 16, 1990 and t is the number of days since April 24, 1990 (HST launch). If the desorption continues along the present curve, focus will be maintained within 3 microns of the October 18, 1991 until the next move planned in August 1993.

As the focus has been stable since the November 1992 mirror move, an observer should not expect a change in focus error of more than 1/20 th wave at 6328 Åin observations made after that date. Any focus variation is due to OTA "breathing" and does not have a major impact on PSFs used for deconvolution. The period between April 1991 and August 1992 has seen the largest focus variations (on the time scale of several months differences in focus corresponding to secondary mirror positions which differ by $10 - 20$ microns occur). For deconvolution of observations taken during this period, observers should choose PSFs judiciously. If observed PSFs are chosen for deconvolution, Figure 6 can be used as a guideline to ensure that the PSF was taken at a date when the secondary mirror was within 5 microns of its position on the date that the data being deconvolved was taken. Simulated PSFs generated for deconvolution purposes should be computed at the focus position on the date of the observation.

The cause for OTA breathing is under investigation, there being some indication that it is thermally induced. Over an orbital period focus variations of $\sim 3 - 5$ microns may occur and would not significantly degrade HST images even after the refurbishment mission. Long term focus variations of $\sim 3 - 15$ microns have been noticed and are expected to be pointing dependent.

We would like to thank Ralph Bohlin for reviewing the manuscript and making useful suggestions.

REFERENCES

Bevington, R. P., 1969, Data Reduction and Error Analysis for the Physical Sciences, (New York:McGraw-Hill), p. 235.

Born, M. and Wolf, E. 1965, Principles of Optics, 3rd Ed. (Oxford, London, Edinburgh, New York, Paris, Frankfurt: Pergamon Press), p. 464.

Burrows, C. J., Holtzman, J. A., Faber, S. M., Bely, P. Y., Hasan, H., Lynds, C. R. and Schroeder, D. 1990, ApJ, 369, L21.

Jedrzejewski, R., 1991, in Optical Alignment Panel Final Report, December 1991.

Schroeder, D., 1987, Astronomical Optics (San Diego:Academic Press), p 20.

Schroeder, D., 1991, Optical Alignment Panel Final Report, December 1991.

Zernike, F., 1934, Physica, 1, 689.

Table 1.

All scientifically relevant OTA secondary mirror moves since launch

			Secondary Position					
Yr	Day	Date/Time (GMT)	DX +V1	DY +V3	DZ +V2	TX −OV1	TY +OV2	TZ −OV3
			μm	*μm*	*μm*	*arcseconds*		
90	114	LAUNCH	0	0	0	0	0	0
90	140	20-May-90 08:20	−615	0	0	0	0	0
90	166	15-Jun-90 10:50	−690	−392	152	0	−212	133
90	176	25-Jun-90 21:36	−539	0	0	−1	0	0
90	204	23-Jul-90 07:42	−711	−129	304	0	−86	61
90	227	15-Aug-90 18:09	−701	−377	537	1	−170	140
90	299	26-Oct-90 15:08	−681	−377	537	1	−170	140
90	351	17-Dec-90 01:36	−680	−109	281	1	−79	53
91	053	22-Feb-91 14:50	−655	−109	281	1	−79	53
91	081	22-Mar-91 14:06	−655	153	19	1	−79	53
91	096	06-Apr-91 22:22	−655	−109	281	1	−79	53
91	101	11-Apr-91 22:26	−640	−109	281	1	−79	53
92	236	23-Aug-92 23:37	−626	−109	281	1	−79	53
92	330	25-Nov-92 12:46	−616	−109	281	1	−79	53

Table 2.

Average pad circle radius $< r >$ vs. $\Delta(SM)$

$\Delta(SM)$	$< r >$	$\Delta(PF)$	$< r >$
μm	μm	mm	FOC *pixels*
0	596.5	0	87.57
100	396.8	10.97	58.25
200	197.0	21.92	28.92

Table 3.

Comparison of $\Delta(SM)$ using Pad Method and Phase Retrieval Method

True	OPD (HH)	Ray Trace (HH)	Ray Trace (DJS)	Phase Retrieval
105.9	111.7	113.4		104.7
100.9	108.1	109.6		100.4
	123.7	125.2	123	117.5
	111.6	112.6	114	107.7
	105.3	106.1	110	95.4

Table 4.

Desorption of secondary mirror as measured by the pad method.

Date	Days since launch	Microns measured
16-Aug-90	114	0.0
24-Oct-90	183	21.0
21-Nov-90	211	31.0
17-Dec-90	237	27.0
2-Feb-91	284	38.0
30-Apr-91	371	50.0
26-May-91	397	47.0
24-Aug-91	487	56.0
17-Sep-91	511	54.0
20-Nov-91	575	60.0
17-Mar-92	693	72.0
19-May-92	756	70.9
6-Oct-92	896	77.7
26-Jan-93	1008	82.5

FIGURE CAPTIONS

Figure 1. OTA exit pupil used for constructing model PSFs. The outermost circle represents the OTA primary; the inner circle represents the central obscuration the baffle supporting the OTA secondary mirror. The three small circles labeled 1, 2 and 3 are obscurations caused by the pads supporting the primary mirror. The four rectangular obscurations are caused by the spiders supporting the OTA secondary. The OTA axes (V2, V3) are shown.

Figure 2. A schematic diagram showing the relation between the pupil image at paraxial focus and at a distance $\Delta(PF)$ from paraxial focus. Rays through the centers of the three pads are shown proceeding from paraxial focus to the image plane. The pad radii measured on the image are denoted by r_1, r_2, r_3.

Figure 3. Desorption measurements and the best fit curves for FOC data available till November 20, 1991 (dashed curve), May 19, 1992 (dot-dash curve) and current best fit (solid curve). There is a large difference between the curves beyond November 20, 1991.

Figure 4. Desorption measurements from PC observations through filter F439W overplotted with measurements from FOC data through filter 486N. The best fit curve, the equation for which is given at the top of the diagram, is plotted as a solid line. Because of the large discrepancy seen between the WF and PC data on November 4, 1992, PC data through filter through filter F555W was analyzed and is also plotted.

Figure 5. Desorption measurements from WF observations through filter F439W overplot-

ted with measurements from FOC data through filter 486N. The best fit curve, the equation for which is given at the top of the diagram, is plotted as a solid line. Because of the large discrepancy seen between the WF and PC data on November 4, 1992, WF data through filter through filter F555W was analyzed and is also plotted.

Figure 6. Reference position for October 18, 1991 as well as the mirror moves made to counter desorption are indicated on the plot. The FOC and PC data are overplotted together with the desorption curve (dashed lines). Also overplotted here are the results of measurements on the 34 images taken in the CVZ through filter F555W on December 25, 1992. In the past, large excursions from the October 18, 1991 position have occurred, though the focus has stabilized since the November 1992 mirror move. When choosing PSFs for deconvolution the focus changes on a time scale of months should be taken into account.

Figure 7. Reference position for October 18, 1991 as well as the mirror moves made to counter desorption are indicated on the plot. The FOC and WF data are overplotted together with the desorption curve (dashed lines).

Figure 8. Differences in $\Delta(SM)$ obtained from measurements and the best fit (desorption) curve for WFPC stellar monitoring data.

Figure 9. Variation of $\Delta(SM)$ over 5 complete orbital cycles and two partial cycles. The measurements for each cycle are denoted by a different symbol and connected by different linestyles. The lines are a guide to the eye.

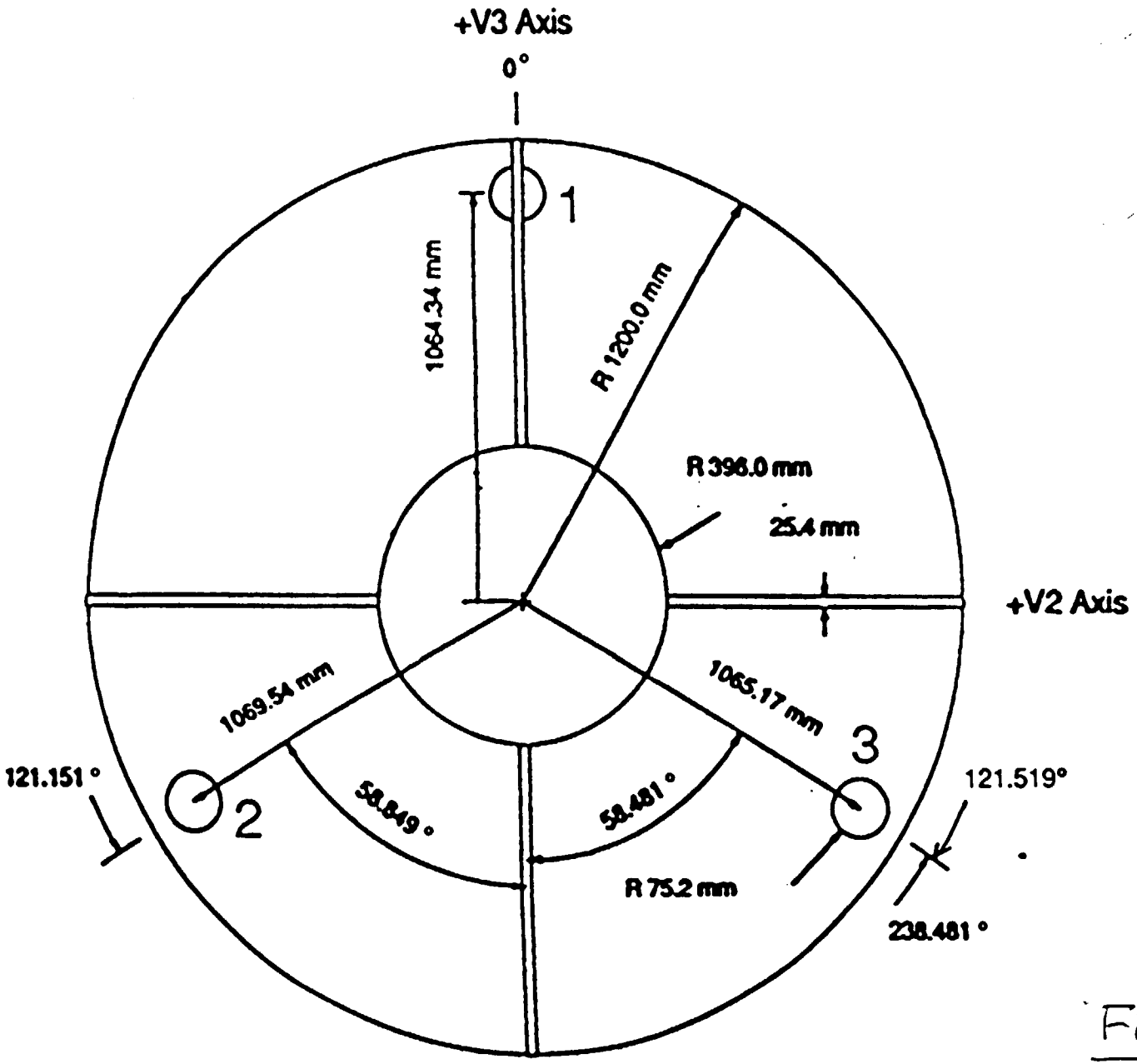
+V3 Axis
0°
1
1064.34 mm
R 1200.0 mm
R 396.0 mm
25.4 mm
+V2 Axis
1069.54 mm
1065.17 mm
3
121.151°
2
58.849°
58.481°
121.519°
R 75.2 mm
238.481°

Fig 1

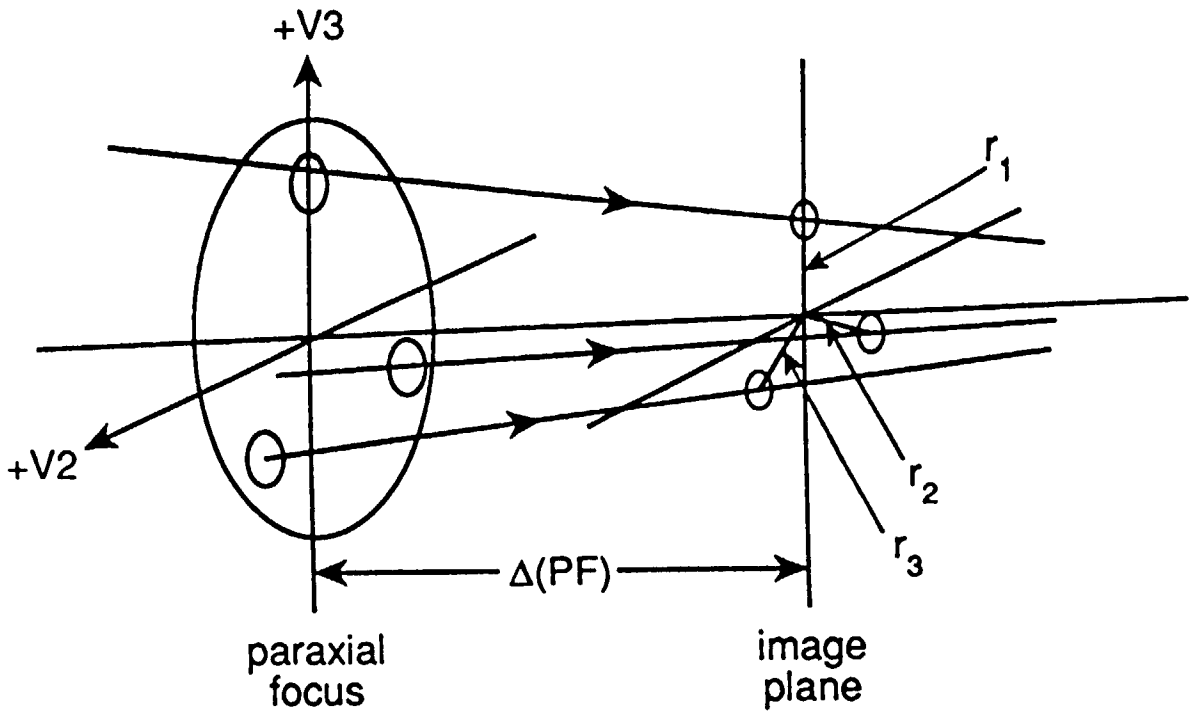

Fig 2

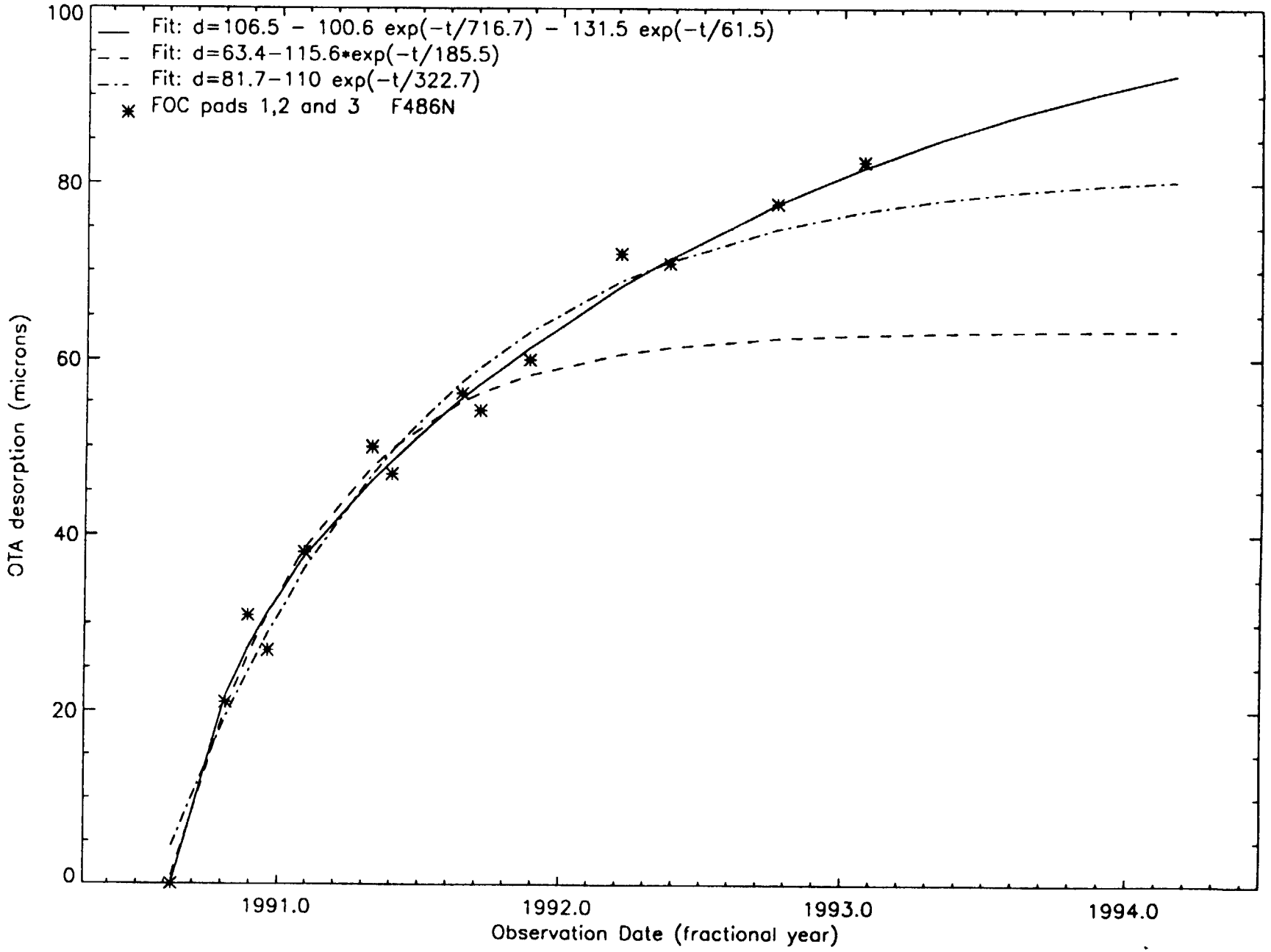
Fit: d=106.5 - 100.6 exp(-t/716.7) - 131.5 exp(-t/61.5)
Fit: d=63.4-115.6*exp(-t/185.5)
Fit: d=81.7-110 exp(-t/322.7)
FOC pads 1,2 and 3 F486N
OTA desorption (microns)
0
20
40
60
80
100
1991.0
1992.0
1993.0
1994.0
Observation Date (fractional year)

Fig 3

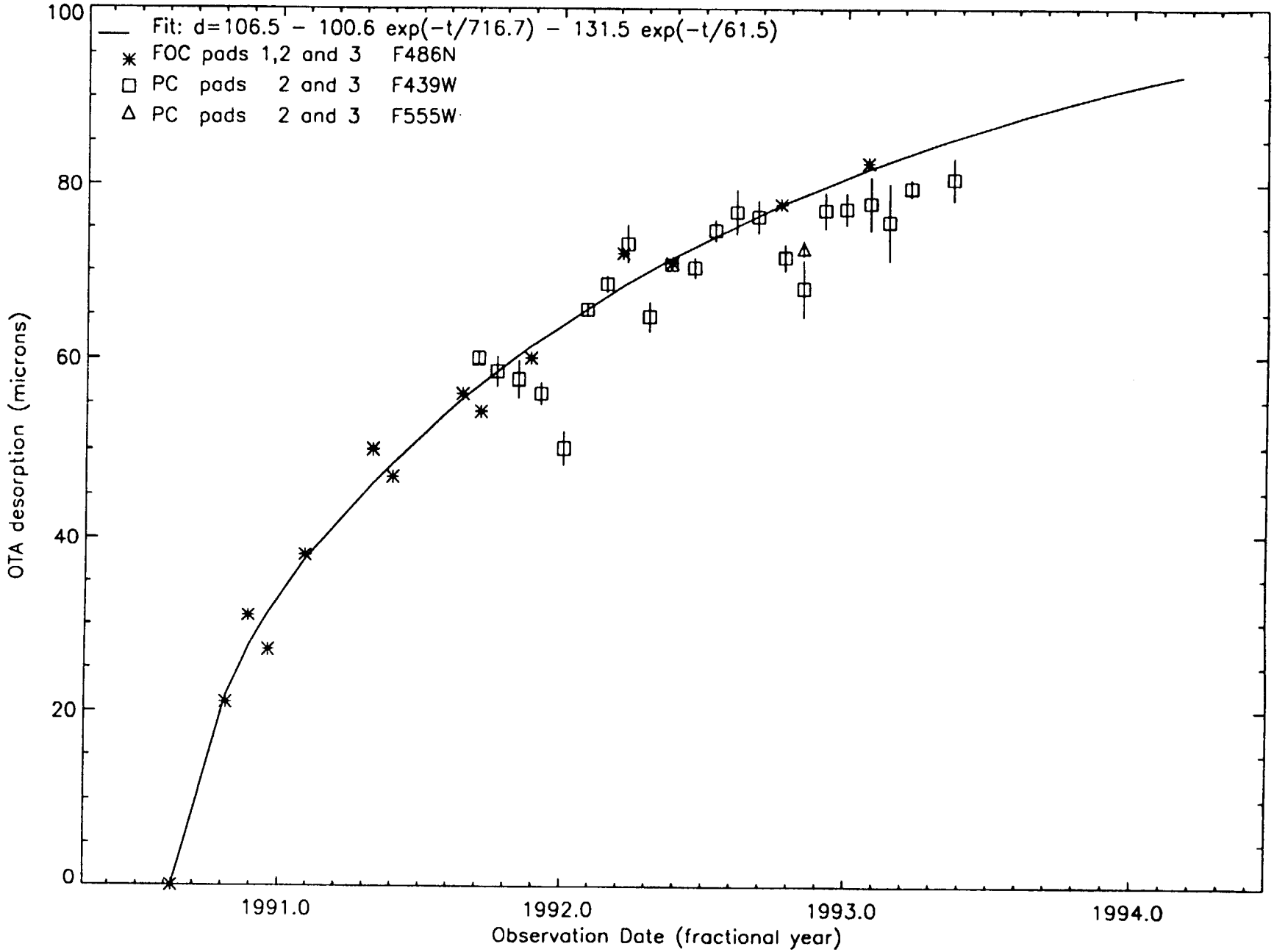
Fit: d=106.5 − 100.6 exp(−t/716.7) − 131.5 exp(−t/61.5)
FOC pads 1,2 and 3 F486N
PC pads 2 and 3 F439W
PC pads 2 and 3 F555W
OTA desorption (microns)
0
20
40
60
80
100
1991.0
1992.0
1993.0
1994.0
Observation Date (fractional year)

Fig 4

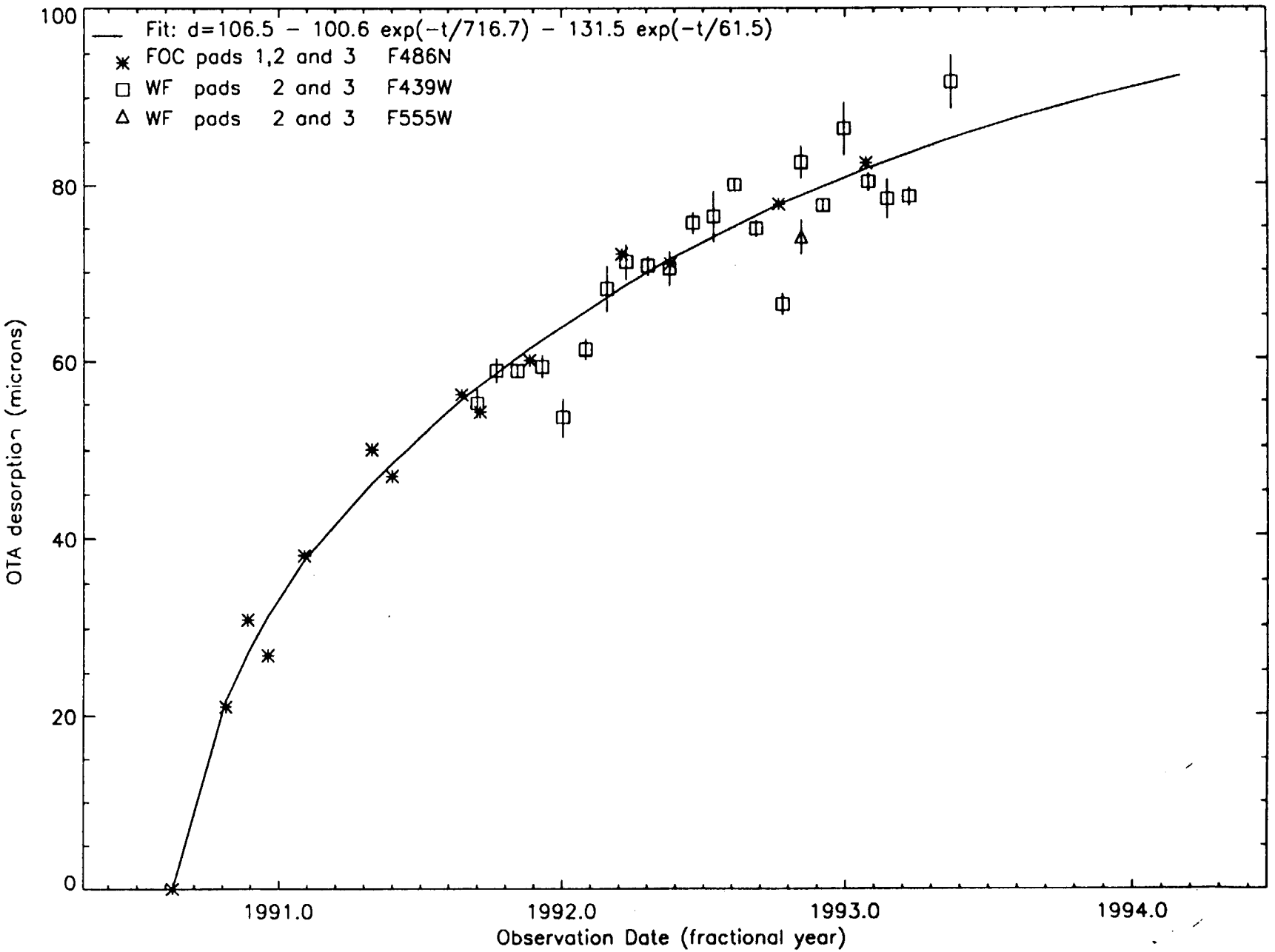
Fit: d=106.5 − 100.6 exp(−t/716.7) − 131.5 exp(−t/61.5)
FOC pads 1,2 and 3 F486N
WF pads 2 and 3 F439W
WF pads 2 and 3 F555W
OTA desorption (microns)
Observation Date (fractional year)
0
20
40
60
80
100
1991.0
1992.0
1993.0
1994.0

Fig 5

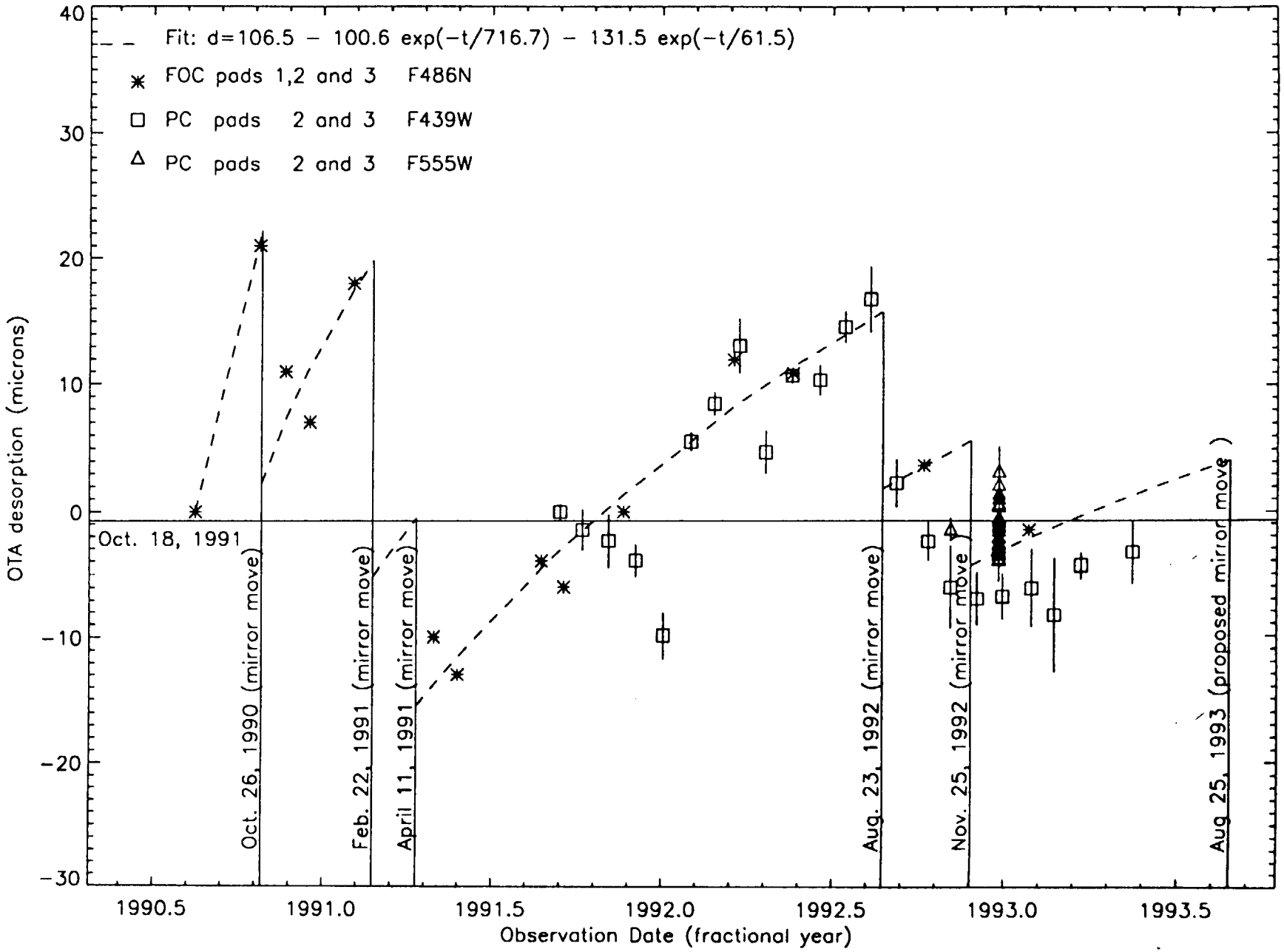
Fit: d=106.5 − 100.6 exp(−t/716.7) − 131.5 exp(−t/61.5)
FOC pads 1,2 and 3 F486N
PC pads 2 and 3 F439W
PC pads 2 and 3 F555W
OTA desorption (microns)
Observation Date (fractional year)
Oct. 18, 1991
Oct. 26, 1990 (mirror move)
Feb. 22, 1991 (mirror move)
April 11, 1991 (mirror move)
Aug. 23, 1992 (mirror move)
Nov. 25, 1992 (mirror move)
Aug 25, 1993 (proposed mirror move)
40
30
20
10
0
−10
−20
−30
1990.5
1991.0
1991.5
1992.0
1992.5
1993.0
1993.5

Fig 6

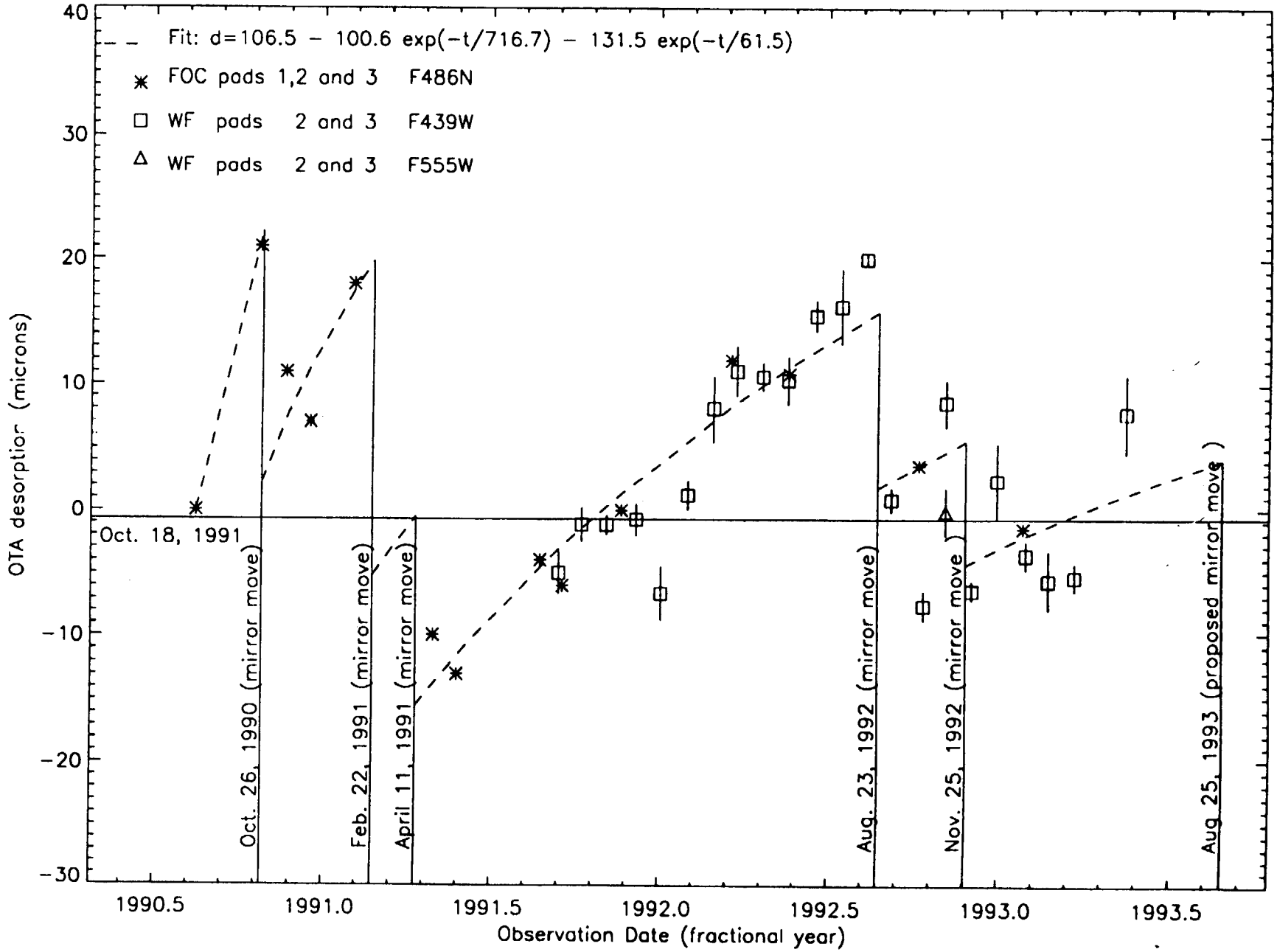
Fit: d=106.5 − 100.6 exp(−t/716.7) − 131.5 exp(−t/61.5)
FOC pads 1,2 and 3 F486N
WF pads 2 and 3 F439W
WF pads 2 and 3 F555W
OTA desorption (microns)
Observation Date (fractional year)
Oct. 18, 1991
Oct. 26, 1990 (mirror move)
Feb. 22, 1991 (mirror move)
April 11, 1991 (mirror move)
Aug. 23, 1992 (mirror move)
Nov. 25, 1992 (mirror move)
Aug 25, 1993 (proposed mirror move)
40
30
20
10
0
−10
−20
−30
1990.5
1991.0
1991.5
1992.0
1992.5
1993.0
1993.5

Fig 7

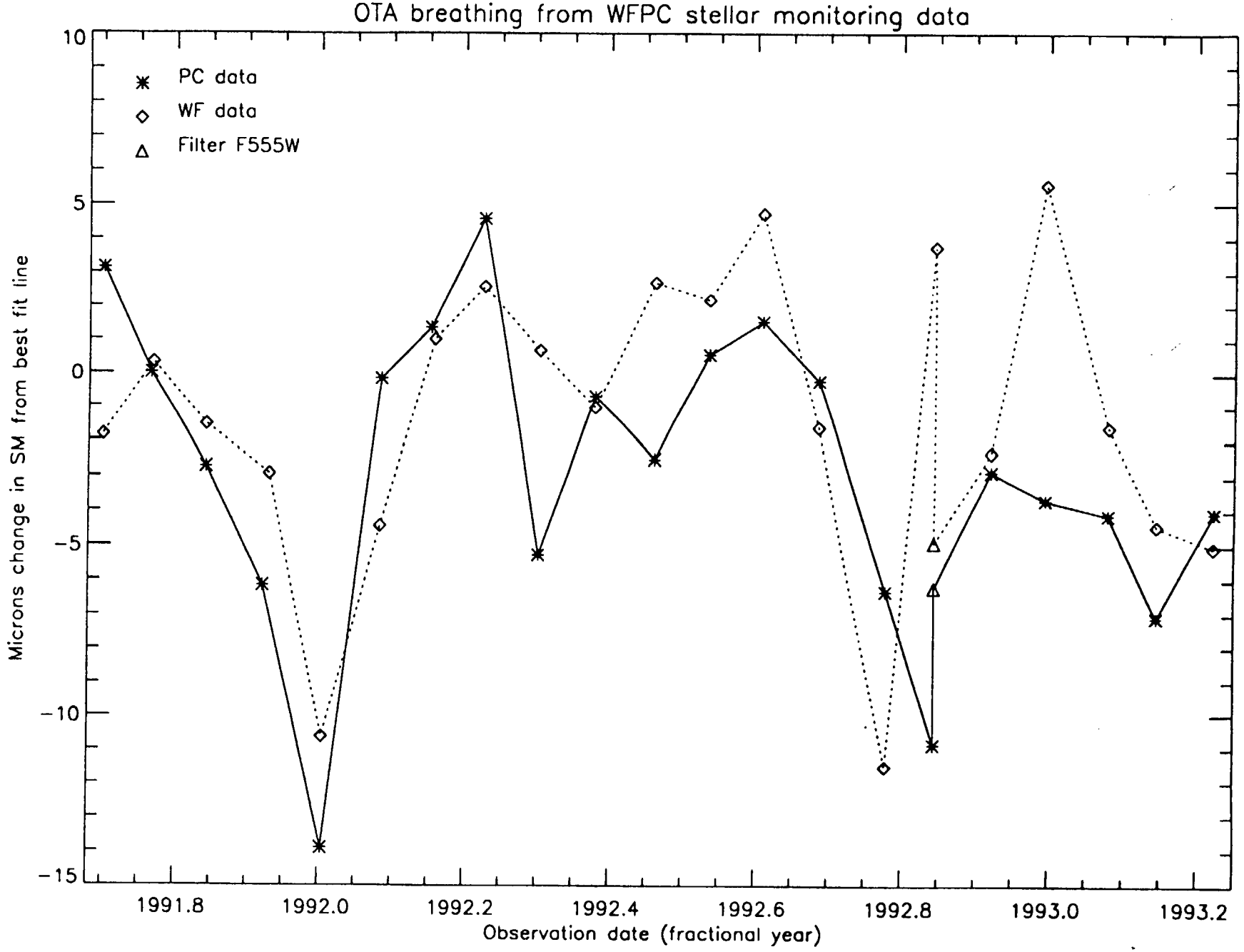
OTA breathing from WFPC stellar monitoring data
PC data
WF data
Filter F555W
Microns change in SM from best fit line
Observation date (fractional year)
10
5
0
−5
−10
−15
1991.8
1992.0
1992.2
1992.4
1992.6
1992.8
1993.0
1993.2

Fig 8

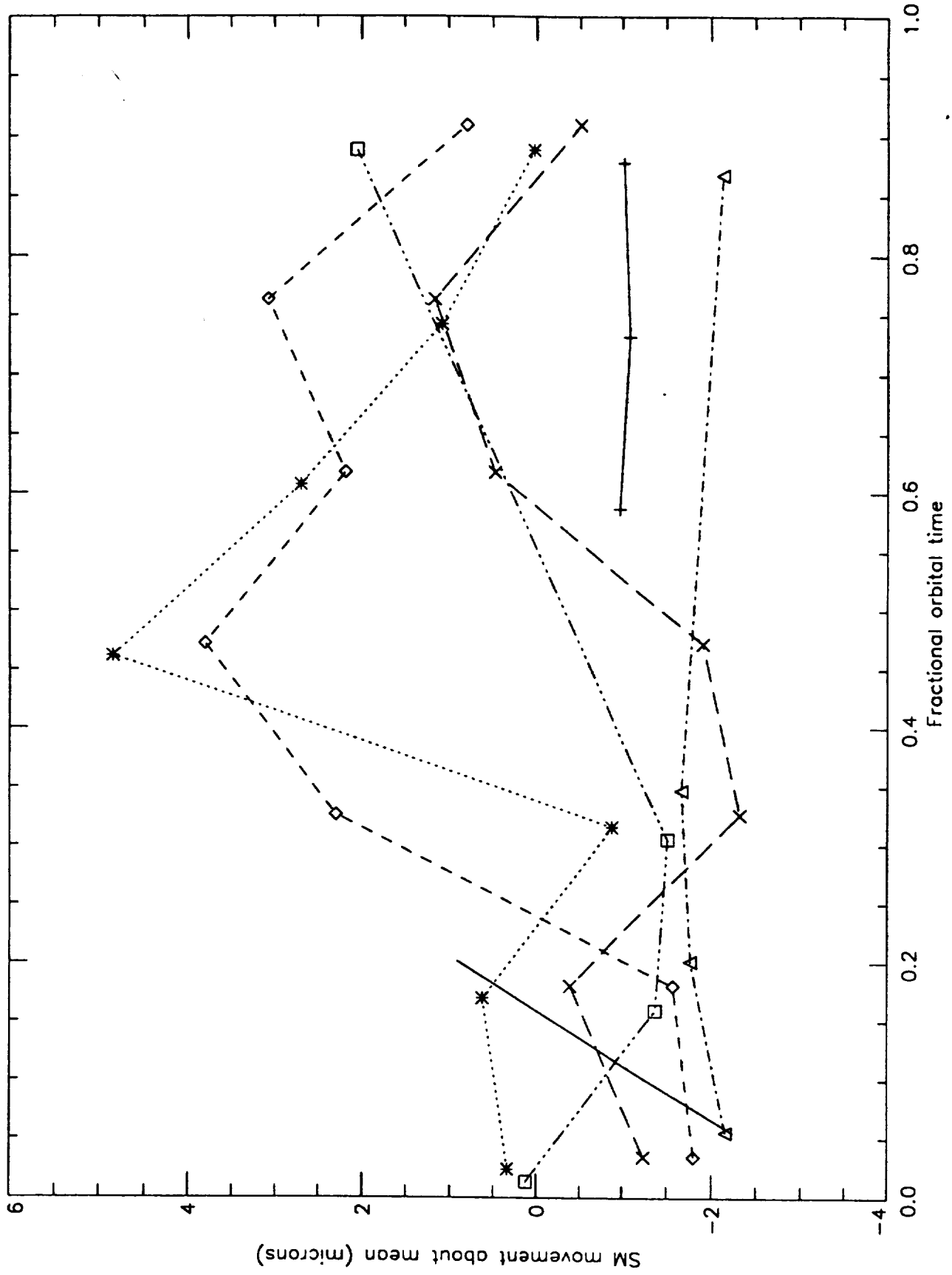
SM movement about mean (microns)
6
4
2
0
-2
-4
0.0
0.2
0.4
0.6
0.8
1.0
Fractional orbital time

Fig 9

Defocus – OTA / Axial cameras

Following are some relations appropriate for the OTA with extensions to include axial cameras. First for some definitions:

w = rms wavefront error

$w(\mu)$ = w in microns

$w(\lambda)$ = w in number of waves, hence dimensionless

ΔZ = shift from diffraction focus

F = focal ratio = 24 for OTA, F_c for camera

$\varepsilon = 0.33$

$$w = \frac{(1-\varepsilon^2)}{16\sqrt{3}\,F^2}\,\Delta Z$$

$$w(\mu) = 0.0558\,\Delta Z(\text{mm})$$

$$w(\lambda) = \frac{0.0558}{\lambda(\mu)}\cdot\Delta Z(\text{mm})$$

In terms of geometric blur dia, as shown in the sketch, we have

$$d = \Delta Z/F$$

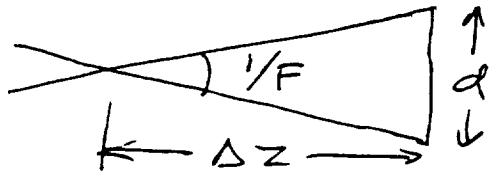

If ΔSM = axial shift of secondary mirror, then

$$\Delta Z = 110 \cdot \Delta SM.$$

For camera of final focal ratio F_c, we have

$$\Delta z_c = m^2 \Delta z, \quad d_c = md,$$

where $m = F_c/24$.

∴ distance from diffraction focus $\propto F_c^2$, diameter (in linear terms) of defocus blur $\propto F_c$.
Wavefront error $w_c = w$, because error is not changed by simple reimaging (unless camera is refocused).

$$\text{OTA scale} = 3.58''/\text{mm} = \frac{206265}{FD}$$

$$\text{camera scale} = 3.58\left(\frac{24}{F_c}\right)''/\text{mm}$$

Since linear diameter of blur $\propto F_c$ and camera scale $\propto F_c^{-1}$, the angular diameter of blur is unchanged by simple reimaging.

Geometric blur diameter and Airy disc

Let d = diameter of Airy disc (1st dark ring) for $\mathcal{E} = 0.33$.

∴ $d = 2.2\lambda f/D = 2.2\lambda F$ ($\mathcal{EE} = 65\%$ for perfect system).

$$W = \frac{(1-\varepsilon^2)}{16\sqrt{3}F^2} \cdot Fd = \frac{(1-\varepsilon^2)}{16\sqrt{3}F^2} \cdot 2.2\lambda F^2$$

$$\therefore W(\lambda) = \frac{2.2(1-\varepsilon^2)}{16\sqrt{3}} = 0.071 \Rightarrow \frac{\lambda}{14} \text{ focus error}$$

Assume $\Delta SM = 5\mu$, hence $\Delta Z = 0.55$ mm.
Let $\alpha = d/f$ = angular blur. Results for selected λ's are as follows.

λ (nm)	$\alpha(\pi)$	$\alpha_{Def}(\pi)$	
400	0.076	0.082	} $\Delta SM = 5\mu$
600	0.113	0.082	
800	0.151	0.082	

↑ dia of 1st dark ring

For $\Delta Z = 0.55$ mm we find defocus blur = Airy disc diameter for $\lambda = 430$ nm – see graph. For $\lambda > 430$ nm the rms focus error $< \lambda/14$.

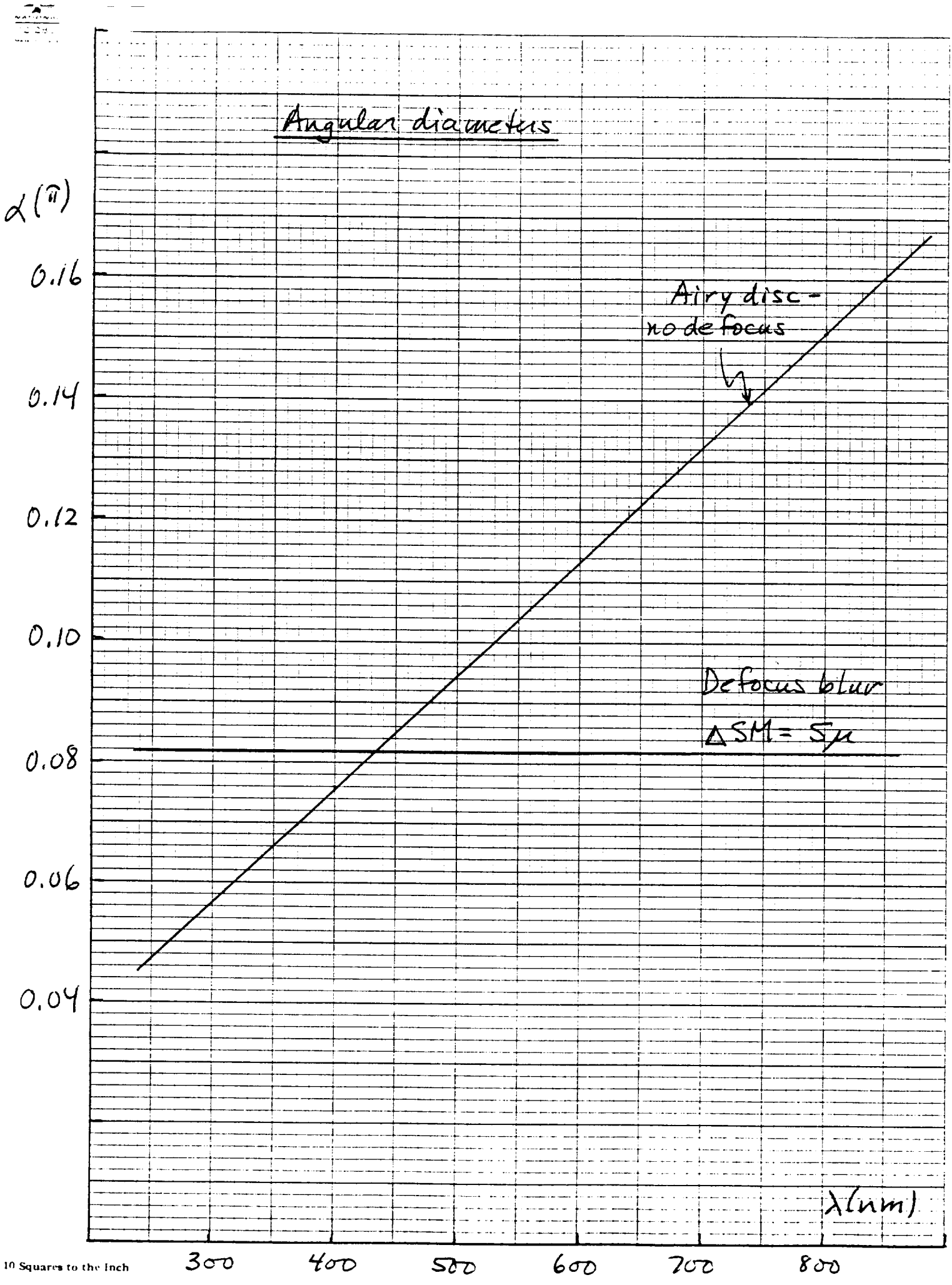

10 Squares to the Inch

Astigmatism - OTA / Axial cameras

$W(\mu) = 0.00197\,\theta^2(')$ = rms astigmatism
W (waves at 633 nm) $= 0.00311\,\theta^2(')$

$AAS(") = 0.00313\,\theta^2(')$ = dia of astigmatic blur circle

$\theta(')$	$W(\mu)$	$AAS(")$
5.4	0.0574	0.092
5.7	0.0640	0.102
6.0	0.0709	0.113
6.3	0.0782	0.124
6.6	0.0858	0.136
6.9	0.0938	0.149
7.2	0.1021	0.162
7.5	0.1108	0.176
7.8	0.1200	0.191
8.1	0.1293	0.205

$AAS(") = 1.59\,W(\mu)$

Assume θ_0 = angle at which OTA astigmatism is corrected by axial camera (AC).

$W_{residual} = W_r = W - W_0 = 0.00197(\theta^2 - \theta_0^2)$.
For $\theta_0 = 5.7'$ (angle chosen for f/36 AC), take difference between line and curve on graph.

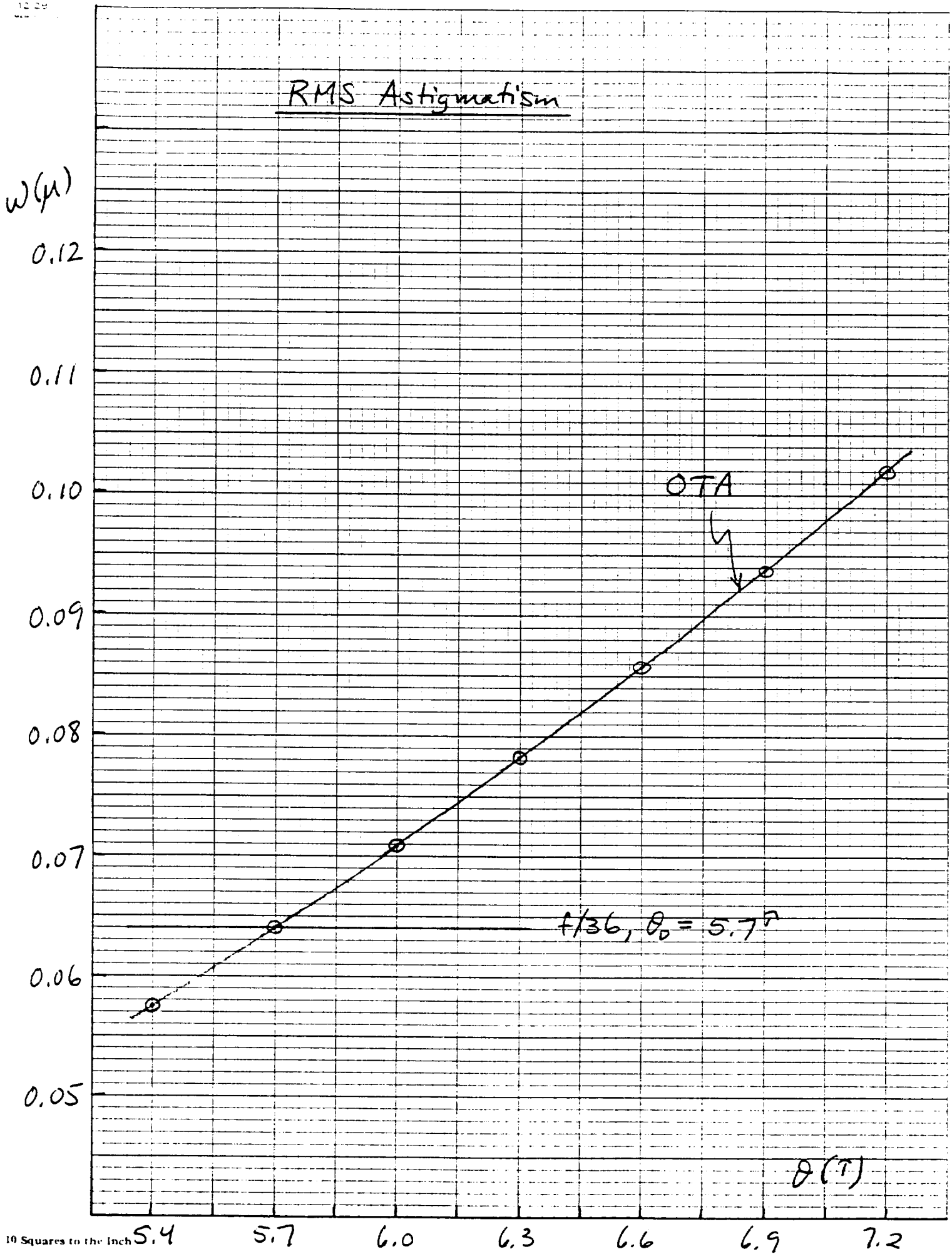
RMS Astigmatism
w(μ)
0.12
0.11
0.10
0.09
0.08
0.07
0.06
0.05
OTA
f/36, θ₀ = 5.7°
θ(T)
5.4
5.7
6.0
6.3
6.6
6.9
7.2
10 Squares to the Inch

Results for f/36 AC

Any 2-mirror AC contributes astig which can add to or subtract from the residual OTA astigmatism. The results to follow are gleaned from ray traces of an f/36 AC with $\theta_0 = 5.7^\circ$ and angles within the AC chosen to reduce coma to negligible values.

Coordinate system, as viewed looking at PM of OTA, is shown at right. Center plane of AC is along horizontal line. OTA astig varies with θ_x, not θ_y (over small angles).

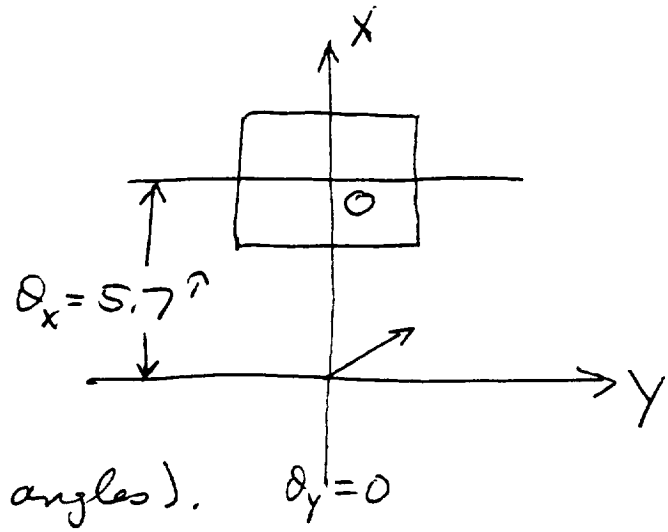

Center of field $O = (5.7^\circ, 0)$.
Diameter of blur at circle of least confusion is plotted on the following graph, where $\underline{d}$ is diameter of circle enclosing all or nearly all of the rays.
Dia d = 5x rms radius (given under spot patterns).

Camera scale $= 3.58\left(\frac{24}{36}\right) = 2.39''/\text{mm}$.

$\therefore AAS('') = 0.00239\, d(\mu)$

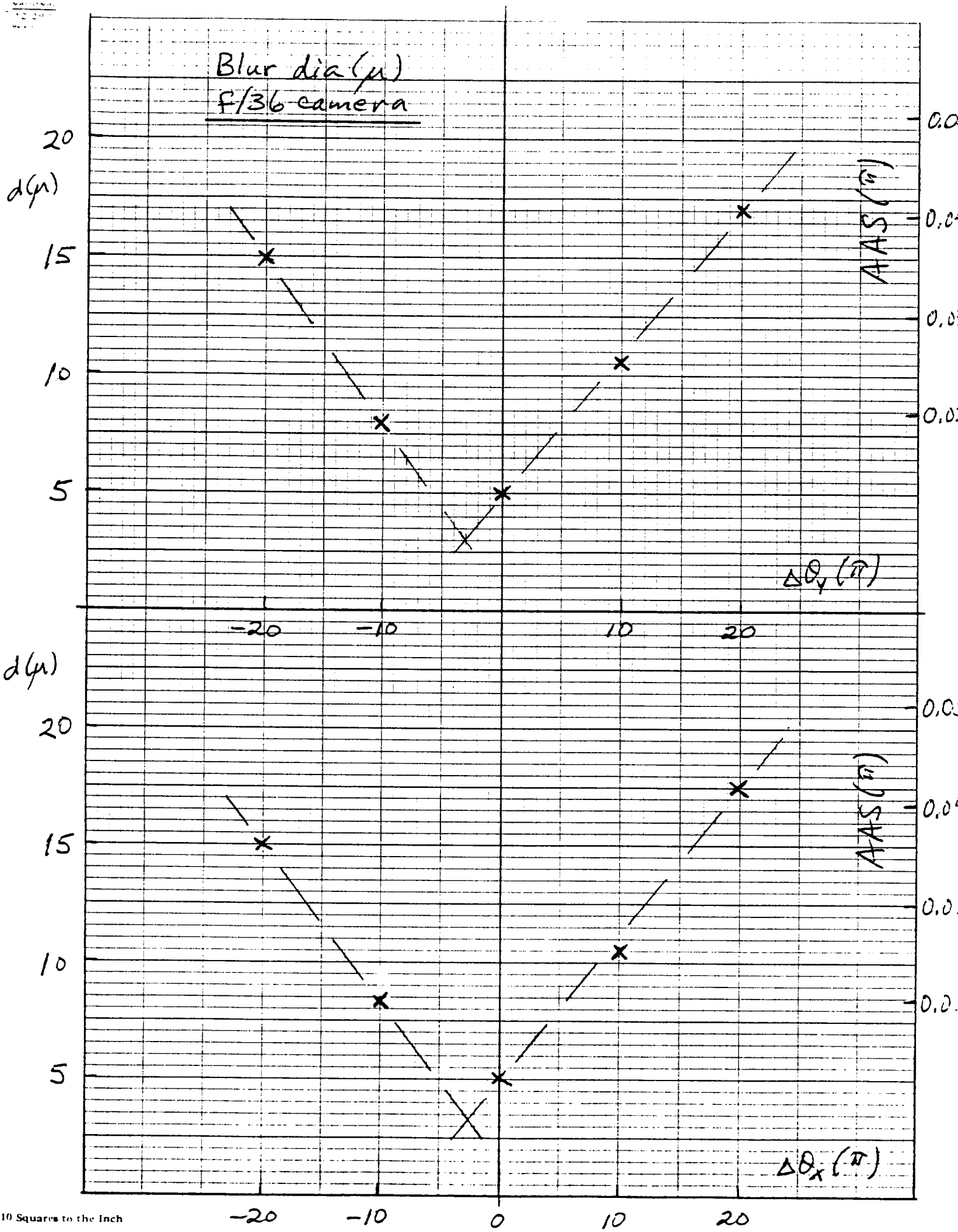
Blur dia (μ)
f/36 camera
d(μ)
20
15
10
5
-20
-10
10
20
ΔθY (π)
AAS (Ω)
0.0
0.0
0.0
0.0
d(μ)
20
15
10
5
-20
-10
0
10
20
ΔθX (π)
AAS (Ω)
0.0
0.0
0.0
0.0

Assuming that the increase in d as $\Delta\theta_x$ or $\Delta\theta_y$ increases is due entirely to astigmatism, we find

$$\frac{\Delta d}{\Delta \theta} = 0.6\mu/''$$

The plot suggests there is a residual spherical aberration still present ($d \simeq 3\mu$), with astig fully corrected a few sec from the center of the field. Subtracting the residual SA, and offsetting to the center of the field, we get

$$d(\mu) = 0.6\,\Delta\theta('')$$

hence

$$AAS('') = 0.00143\,\Delta\theta('').$$

For the OTA only we find $\Delta AAS('') = 0.00626\,\theta\,\Delta\theta$, where both angles are in $'$. Changing $\Delta\theta$ to units of $''$ we find $\Delta AAS('') = 0.00059\,\Delta\theta('')$, for $\theta = 5.7'$. Hence the main contributor to the astigmatism in the OTA/AC combination is the camera, not the OTA.

Note that w(waves at 633 nm) $\simeq$ AAS($''$). Setting AAS = $0.05''$ we find $\Delta\theta = 35''$.

$\therefore$ $W(\lambda = 633) < \lambda/20$ over a square 50 x 50 arcsec field, at 633 nm. For λ = 400 nm, the $\lambda/20$ limit holds for a $32 \times 32''$ field.

May 1993
Dan Schroeder

MANAGEMENT: DOCUMENT STATUS SCREEN

DOC NUMBER 186020 FILE: 1N ACCESSION: 0 ISSUE: 0

HAS BEEN IN IPS SINCE 19931006 (FOR 94 DAYS)

IT HAS BEEN IN THE ABST QUEUE SINCE 19931008 AT 1900

SUBQUEUE OWNER IS SINCE 0 AT 0

LAST ACTION BY	KCG	ON 19931008	AT 802
EVALUATED BY	PNF	ON 19931006	
CATALOGED BY	KCG	ON 19931008	
DUPE-CHECKED BY		ON 19931008	
ABSTR. ENTERED BY		ON 0	
ABSTR. INDEXED BY		ON 0	
QASS REVIEWED BY		ON 0	
REPRO ADVANCED BY		ON 0	

SNAP(QUEUE: _____ SUBQUEUE: _____ PROB: _ DOC NR: _____)

PF1=HELP; PF3=SELECTION SCREEN

4B• A =-•PC LINE 39 COL 19